

Universality of Alpha-Relaxation in Glasses

Valeriy V. Ginzburg¹, Oleg Gendelman², Riccardo Casalini³, and Alessio Zaccone⁴

¹Department of Chemical Engineering and Materials Science, Michigan State University,
East Lansing, Michigan, USA 48824

²Faculty of Mechanical Engineering, Technion, Haifa 32000003, Israel

³Chemistry Division, Naval Research Laboratory, 4555 Overlook Avenue SW, Washington, D.C.,
USA 20375

⁴University of Milan, Department of Physics, via Celoria 16, 20133 Milano, Italy

ABSTRACT. In the vicinity of the glass transition, the characteristic relaxation time (e.g., the α -relaxation time in dielectric spectroscopy) of a glass-former exhibits a strongly super-Arrhenius temperature dependence, as compared to the classical Arrhenius behavior at high temperatures. A comprehensive description of both regions thus requires five parameters. Here, we demonstrate that many glass-formers exhibit a universal scaling, with only two material-specific parameters setting the timescale and the temperature scale; the other three being universal constants. Furthermore, we show that the master curve can be described by the recently developed two-state, two-(time) scale (TS2) theory (Soft Matter **2020**, *16*, 810) and regress the universal TS2 parameters. We also show the connection between the TS2 model and the Hall-Wolynes elastic relaxation theory.

Introduction. Glass transition is a phenomenon ubiquitous for many classes of amorphous materials (networks, colloids, molecular fluids, polymers, etc.) [1–12] While there are multiple manifestations of the glass transition, the one most commonly discussed is the super-Arrhenius dependence of the α -relaxation time or viscosity on the temperature. This behavior is often described using the Vogel-Fulcher-Tammann-Hesse [13–15] (VFTH) equation, $\log(\tau[T]) = \log(\tau_\infty) + D/(T - T_0)$, and usually explained on the basis of vanishing configurational entropy [16] or vanishing free volume. [17] Notably, the VFTH equation predicts that the relaxation time diverges as $T \rightarrow T_0$. This divergence has been questioned by many authors (see, e.g., [18–21]) and several non-divergent models have also been proposed. [22–24] The super-Arrhenius behavior is described by multiple theoretical frameworks, such as dynamic facilitation [25–29], elastic models [8–10], random first-order theory (RFOT) [30,31], mode-coupling theory (MCT) [32–35], elastically collective nonlinear Langevin equation (ECNLE) [36,37], and many others. By combining the relaxation time dynamics with equation of state, one can simultaneously model the dielectric relaxation and the volumetric or calorimetric experiments, see, e.g., Douglas *et al.* [38–40] and Lipson *et al.* [41–43].

Recently, we proposed a simple theoretical framework, the “two-state, two-(time)scale” (TS2) model that is able to capture the relaxation time behavior and describe some other experiments (volume relaxation, stress relaxation, density changes on cooling, etc.). [24,44–48] Yet one challenge was to find a simple and robust model parameterization. Here, we use historical data for a number of network, molecular, and polymeric glasses to demonstrate the universality of the relaxation time dependence and to regress the universal TS2 parameters.

The relaxation master curve. In Figure 1, Angell plots [1] are shown for the dielectric α -relaxation times of selected polymer glasses (a) and viscosities of selected network glasses (b). The slope of the curve at the point $T_g/T = 1$ is termed fragility, m ,

$$m = \left. \frac{d \log Y}{d \left(\frac{T_g}{T} \right)} \right|_{\frac{T_g}{T}=1} \quad (1)$$

Here, $Y = \eta$ or τ_α , and T_g is defined as the temperature for which $\eta = 10^{12}$ Pa·s or $\tau_\alpha = \tau_g = 10^2$ s. Most polymers have fragilities in the range ~50 - 200 [49] (Figure 1a). Among the molecular and network glasses, silica has the lowest fragility ($m \sim 20$) and exhibits Arrhenius behavior; other non-polymeric glass-formers have fragilities in a very broad range. The temperature dependence of the relaxation time in the VFTH regime can be conveniently written as,

$$\log \left(\frac{\tau_\alpha[T]}{\tau_\infty} \right) = \frac{K^2}{K + m \left(\frac{T}{T_g} - 1 \right)} \quad (2)$$

where $K = \log(\tau_g/\tau_\infty)$, and $\tau_\infty = 10^{-13}$ – 10^{-11} s. [50–52]

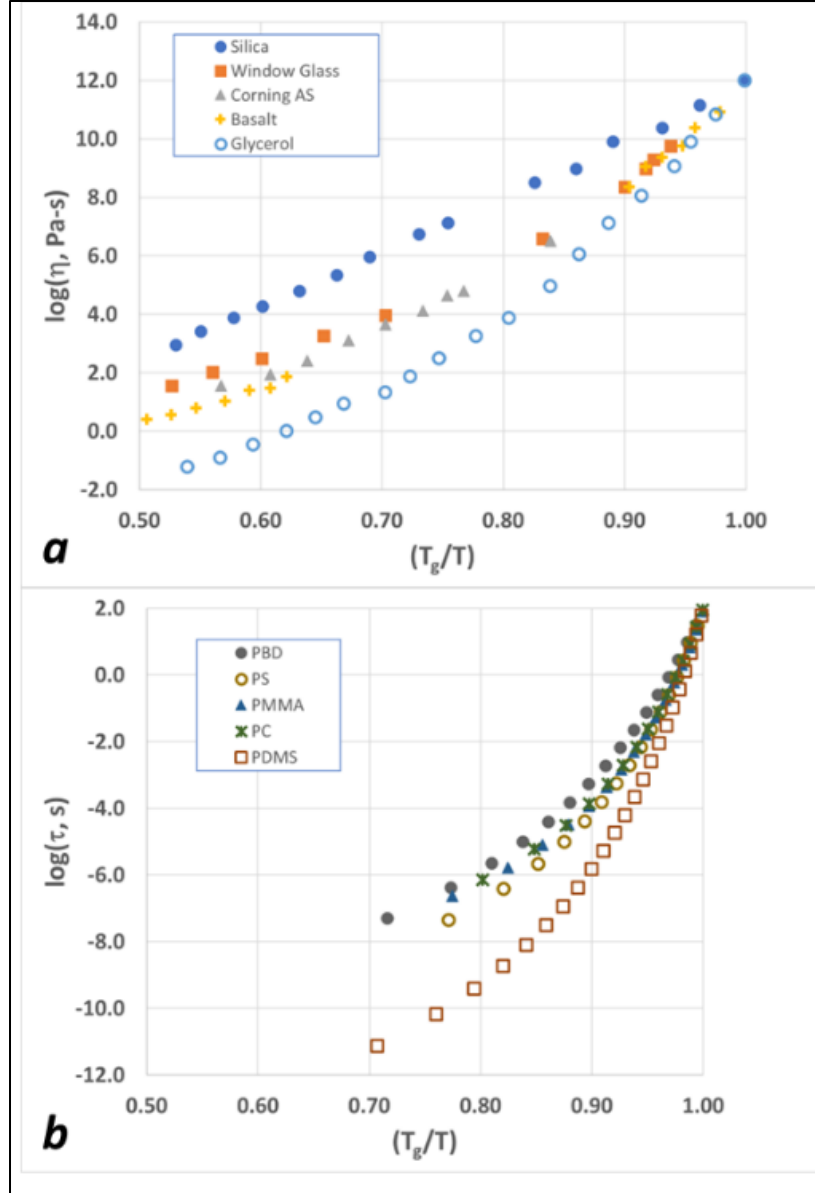


Figure 1. Angell plots: (a) viscosities of several network and molecular glasses (data from Ref. [23]); (b) α -relaxation times of several polymers (data from Refs. [50,53,54]). Abbreviations: Corning AS – Corning aluminosilicate glass; PBD – polybutadiene; PS – polystyrene; PMMA – poly(methylmethacrylate); PC – bisphenol-A polycarbonate; PDMS – poly(dimethyl siloxane).

The Blochowicz equation (2) has three parameters (τ_∞ , m , and T_g). It generally does not describe strong glasses or the high-temperature Arrhenius region for weak glasses and predicts the divergence of the relaxation time as $T \rightarrow T_0 = T_g(1 - K/m)$.

To develop a phenomenological universal description of both strong and fragile glasses in both Arrhenius and VFTH regions, we utilize the combined vertical and horizontal shift procedure similar to the one outlined by Bailly et al. [55] The temperature axis is first converted to logarithmic scale, and then horizontal and vertical shifts are applied to collapse all curves onto a single master curve. (Here, the horizontal shift corresponds to $\ln(T_x/T_g)$ and the vertical shift is $\log(\tau_g/\tau_{el})$; the meaning of the new temperature parameter T_x and time parameter τ_{el} will be discussed below). For our analysis, we use the data for 34 glass-formers, taken from Refs. [50,53,54,56–60] (polymers) and [23,61] (network and molecular glasses); see Table S1 for details. The results for one subset containing 15 materials (3 network glasses, 9 polymer glasses, and 3 molecular glasses) are shown in Figure 2a (log-log plot) and Figure 2b (Arrhenius plot); the other subsets are given in Supporting Information as Figures S1 – S3.

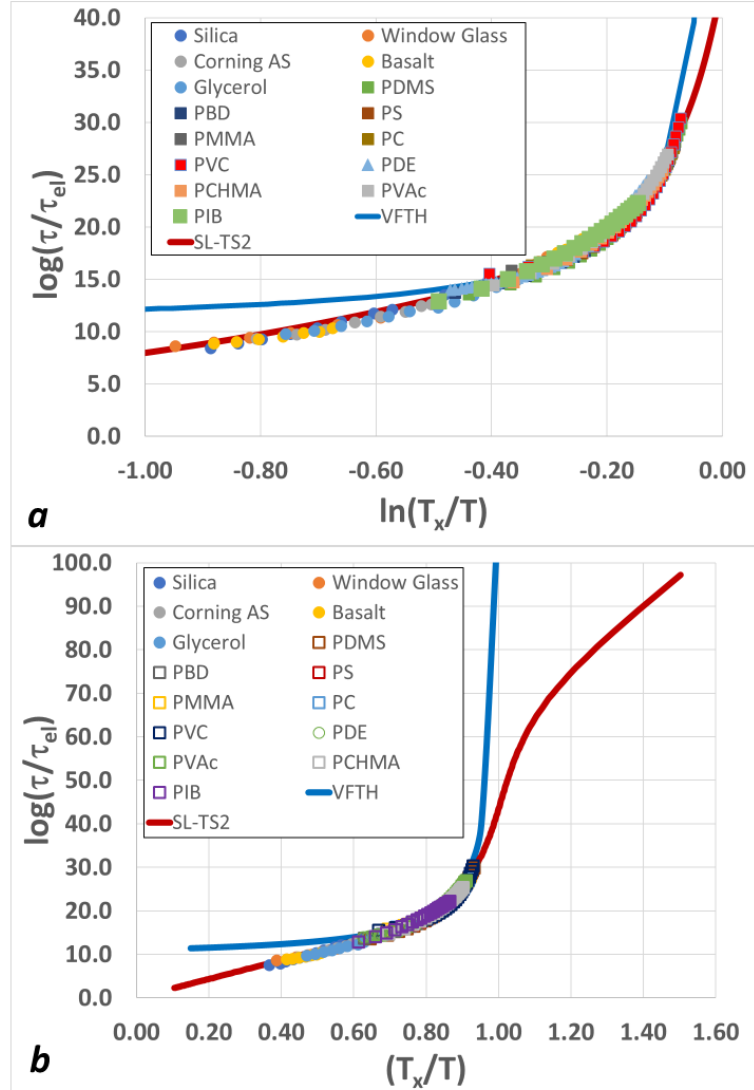


Figure 2. The universal scaling for the α -relaxation and viscosity data for 15 glass-formers. (a) Log-log plot, with details about all the glass-formers used in the modeling. (b) Linear-log plot for the same systems, but with expanded temperature range, extrapolating into the glassy region. The red line corresponds to theoretical SL-TS2 model described below; the blue line is the VFTH fit. Abbreviations: Corning AS – Corning aluminosilicate glass; PDMS – poly(dimethylsiloxane); PBD – polybutadiene; PS – polystyrene; PMMA – poly(methyl methacrylate); PC – bisphenol-A-polycarbonate; PVC – poly(vinylchloride); PDE – phenylphthalen-dimethylether; PVAc – poly(vinylacetate); PCHMA – poly(cyclohexyl methacrylate); PIB – poly(isobutylene).

On the log-log plot (Figure 2a), after the vertical and horizontal shifts, notwithstanding the large difference of the glass formers' fragility, the data collapse onto a single master curve with an Arrhenius region on the left (high temperatures) and a VFTH region on the right (temperatures near T_g). The reference is selected so that when the data are re-plotted in the Arrhenius coordinates (Figure 2b), the

intercept is set to equal to zero. The resulting master curve is successfully (standard deviation of $\log(\tau)$ less than 1.0) fit to the TS2 function,

$$\log\left(\frac{\tau_{\alpha}[X]}{\tau_{el}}\right) = \frac{\bar{E}_1}{X} + \frac{\bar{E}_2 - \bar{E}_1}{X} \psi[X] \quad (3)$$

$$\psi[X] = \left\{1 + \exp\left[\frac{\Delta S}{k_B}(1 - X^{-1})\right]\right\}^{-1} \quad (4)$$

Here, k_B is the Boltzmann's constant, $X = T/T_X$ is the reduced temperature, $\bar{E}_1 = E_1/k_B T_X$, and $\bar{E}_2 = E_2/k_B T_X$ are the reduced activation energies of the “liquid” and “solid” states, respectively, and $\Delta S/k_B$ is the entropy difference between the two states. The timescale τ_{el} is an intrinsic characteristic of the material, although its physical meaning is somewhat uncertain. Equation 4 can be also thought of as an approximate analytical description of the numerical solution to the more fundamental Sanchez-Lacombe two-state, two-(time)scale (SL-TS2) model, given by the minimization of the free energy, [44,46]

$$\begin{aligned} \beta G = & \left[\frac{r}{\nu} \right] \left[\left(\nu \frac{\psi}{r} \right) \ln \left(\nu \frac{\psi r_S}{r} \right) + \left(\nu \frac{1-\psi}{r} \right) \ln \left(\nu \frac{(1-\psi)r_L}{r} \right) + (1-\nu) \ln(1-\nu) \right] \\ & - \frac{\bar{\varepsilon}^*}{X} \left[\frac{r}{\nu} \right] \left[\left(\nu \frac{\psi r_S}{r} \right)^2 + 2\alpha_{SL} \left(\nu \frac{\psi r_S}{r} \right) \left(\nu \frac{(1-\psi)r_L}{r} \right) + \alpha_{LL} \left(\nu \frac{(1-\psi)r_L}{r} \right)^2 \right] \end{aligned} \quad (5)$$

Here, ν is the “occupancy”, z is the lattice coordination number, r_S and r_L are the numbers of lattice sites occupied by the “solid” and “liquid” clusters, respectively; $r = \psi r_S + (1-\psi)r_L$ is the average size of the cooperatively rearranging region (CRR). The normalized energy parameter, $\bar{\varepsilon}^*$, describes the S-S interaction, and the dimensionless parameters α_{LL} and $\alpha_{SL} = \sqrt{\alpha_{LL}}$ describe the relative strength of the

L-L and S-L interactions relative to the S-S one. The universal TS2 and SL-TS2 parameters are summarized in Table S-II.

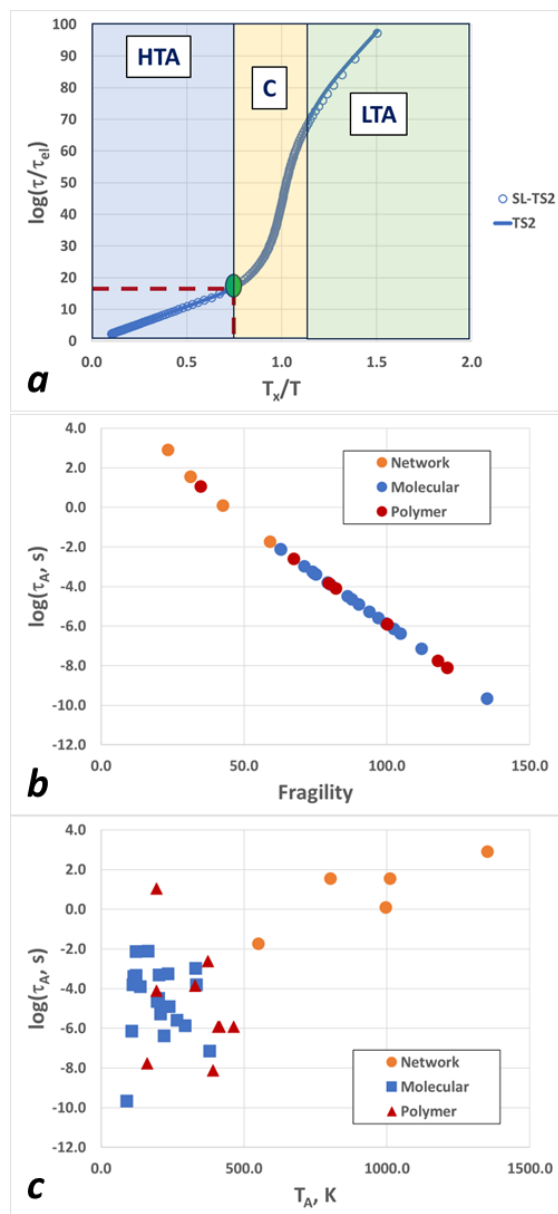


Figure 3. (a) Arrhenius plot for the universal numerical SL-TS2 (circles) and analytical TS2 (solid blue line). The green circle and two red dashed lines describe the Arrhenius temperature and Arrhenius time, as described in the text. Abbreviations: HTA – high-temperature Arrhenius region, C – crossover; LTA – low-temperature Arrhenius region. (b) Logarithm of Arrhenius time vs. fragility for the 34 glass-formers; (c) Logarithm of Arrhenius time vs. Arrhenius temperature.

Arrhenius temperature and Arrhenius time. The “mid-point temperature”, T_x , corresponds to the first-order phase transition between the “liquid” and “solid” states. However, for most materials, $T_x < T_g$; thus, the state of the material at $T = T_x$ is far from equilibrium in any real-life experiment. On the other hand, the glass transition temperature, T_g , does not have thermodynamic meaning – it is simply the point where the “Deborah number” (the ratio of the relaxation time and the experimental time [62]) approaches unity. One convenient way to introduce an accessible yet truly thermodynamic measure of temperature and time was proposed by Douglas and co-workers [63,64] and Simmons and co-workers. [65,66] They emphasized that upon cooling, the relaxation time exhibits a transition from Arrhenius to a super-Arrhenius (“crossover”) behavior, as shown in Figure 3a. Although the transition between the two regions is “fuzzy”, it is possible to define it algorithmically; for example, Simmons et al. [66] defined it as the point where $\log(\tau_\alpha)$ exceeds the Arrhenius extrapolation by 15%. In terms of TS2 or SL-TS2, this translates to the point where $\psi[\overline{T_A}] \equiv \psi_A \approx 0.05$. In other words, the ratio $\overline{T_A} = T_A/T_x \approx 1.23$ is universal, and so is the value of $\log(\tau_A/\tau_{el}) \approx 17.7$ (see the vertical and horizontal red lines in Figure 3a). It is thus straightforward to re-write equations (3) and (4) in terms of ratios (T/T_A) and $\log(\tau_\alpha[T]/\tau_A)$, instead of (T/T_x) and $\log(\tau_\alpha[T]/\tau_{el})$ (see Supporting Information for details).

We can investigate how the Arrhenius temperature and Arrhenius time relate to each other and to the dynamic fragility (Figures 3b and 3c). The logarithm of the Arrhenius time is a nearly perfect linear function of the fragility, with little to no scatter across families (Figure 3b). This is the consequence of the universality we established earlier (see Supporting Information for the functional form of this dependence). The relationship between $\log(\tau_A)$ and T_A (or T_x) is more complicated (Figure 3c). For high-temperature “network glasses” (silica, B_2O_3 , Corning AS, and basalt), there is a clear trend reminiscent of an exponential behavior, $\tau_A(T_A) \cong \tau_A(0) \exp[T_A/H_0]$, where H_0 is some enthalpy parameter. For the polymeric and molecular glasses, however, no such trend emerges and the data are completely scattered.

At this time, we have to conclude that there is no clear “super-universality”, and the two parameters setting the time and temperature scales are independent of each other.

Debye-Waller factor and universality. In their simulations, Simmons et al. [66] discovered that the Debye-Waller factor (mean-square displacement in the super-Arrhenius regime) can be normalized and rescaled to obey a simple temperature dependence,

$$\langle u^2 \rangle_r = \frac{3}{2} T_r - \frac{1}{2}, \quad (6)$$

where $\langle u^2 \rangle_r \equiv \langle u^2(T) \rangle / \langle u^2(T_{ref}) \rangle$ and $T_r \equiv T/T_{ref}$ (see Figure 4a). In their study, Simmons et al. [66] chose $T_{ref} = T_A$; interestingly, we find that equation 6 holds for a relatively broad range of $T_{ref} > T_A$. Let us now consider the relationship between $\log(\tau_r) \equiv \log(\tau[T]/\tau[T_{ref}])$ and $\langle u^2 \rangle_r$. According to elastic activation models (Hall and Wolynes [67], Dyre [9,10], and others), one expects $\log(\tau_r) \propto (\langle u^2 \rangle_r)^{-1} - 1$. We attempt to find T_{ref} for which this expression is valid and agrees with TS2 prediction. First, we re-cast the TS2 formula in terms of T_r and τ_r ,

$$\log(\tau_r) = U_1 \left[\frac{1}{T_r} - 1 \right] + (U_2 - U_1) \left[\frac{1}{T_r} \frac{1}{1 + \exp\left(V \left[\frac{1}{T_r} - \frac{T_{ref}}{T_x} \right]\right)} - \frac{1}{1 + \exp\left(V \left[1 - \frac{T_{ref}}{T_x} \right]\right)} \right] \quad (7)$$

Here, $U_{1,2} = \left(\frac{1}{\ln(10)} \right) \overline{E}_{1,2} \left(\frac{T_x}{T_{ref}} \right)$, and $V = \left(\frac{\Delta S}{k_B} \right) \left(\frac{T_x}{T_{ref}} \right)$. Next, we use equation 6 to express T_r as a function of $\langle u^2 \rangle_r$ and substitute into equation 7. Then, we can vary T_{ref} and compute the dependence of $\log(\tau_r)$ on $w = (\langle u^2 \rangle_r)^{-1} - 1$. In general, this dependence is highly nonlinear, but for $T_{ref} \approx 2.35T_x$, it is well approximated by a straight line. (Note that $T_{ref} \approx 2.35T_x$ is significantly higher than $T_A \approx 1.23T_x$). Figure 4b shows the calculated TS2 line (red) together with a Hall-Wolynes straight line (blue) with the slope of 4.25 (± 0.1). Notably, the simulation data for various glass-formers collapse onto the TS2 or the Hall-Wolynes lines with no free parameters. In effect, given equation 6, this implies that the universal linear dependence of the Debye-Waller factor on the reduced temperature, combined with the universal VFTH-type

approximation for the TS2 function, predicts the universal Hall-Wolynes elastic mechanism of local dynamics and relaxation.

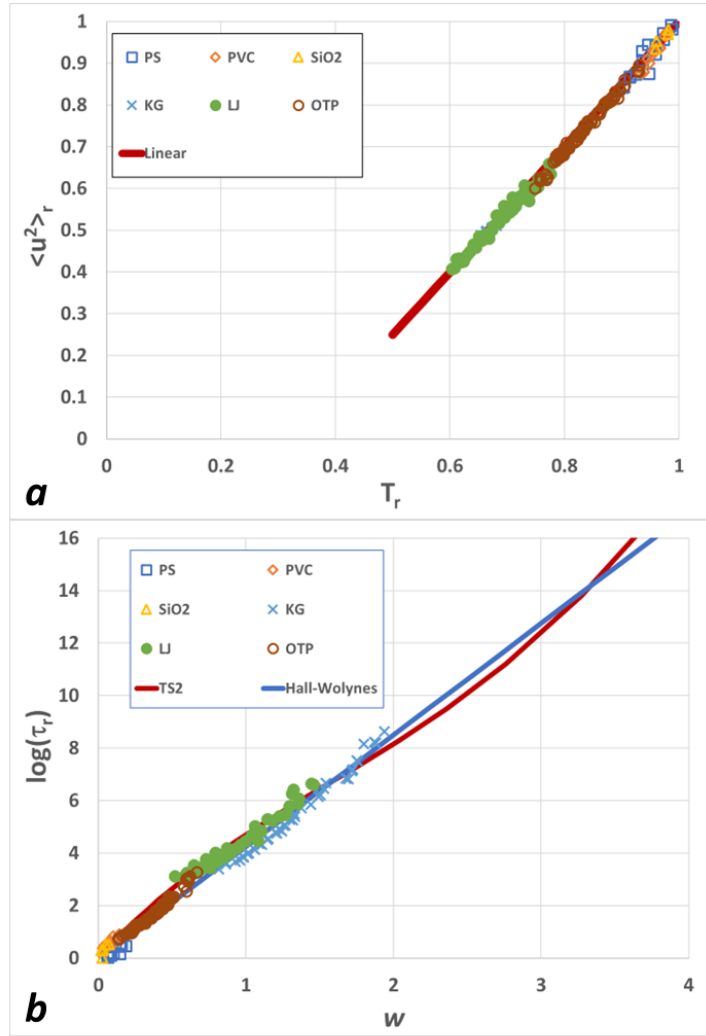


Figure 4. (a) Normalized Debye-Waller factor vs. normalized temperature. Red line – TS2 function; symbols are representative systems from Ref. [66] as shown in the legend. (b) Logarithm of the normalized relaxation time vs. the shifted inverse Debye-Waller factor. Red line – TS2, blue line – elastic model, symbols are representative systems from Ref. [66]. Abbreviations: PS, PVC – all-atom OPLS simulations of 100-mer polystyrene and poly(vinyl chloride); LJ – binary Lennard-Jones; KG – Kremer-Grest polymer, SiO2 – SiO₂ glass; OTP – ortho(terphenyl).

Conclusions. We have demonstrated that the α -relaxation behavior of multiple glass-formers (network, molecular, and polymer) can be successfully captured by a simple two-parameter model, where

the two parameters are the “characteristic material temperature”, T_x , and the “characteristic material time”, τ_{el} . The other, dimensionless, parameters of the master curve (the normalized high-temperature and low-temperature activation energies, $\frac{E_1}{k_B T_X} \approx 50(\pm 3)$ and $\frac{E_2}{k_B T_X} \approx 150(\pm 5)$, and the normalized entropy difference between the liquid and solid states, $\frac{\Delta S}{k_B} \approx 16(\pm 1)$) are universal. We do not yet fully understand the origin of this universality. The knowledge of the relaxation time allows us to predict the nonequilibrium experiments like volume, enthalpy, and stress relaxation, or the specific volume and enthalpy changes upon heating or cooling. Longer-term, these results will help us develop new models for visco-elasto-plastic deformation in amorphous near-glassy materials. These will be subject of future studies.

Acknowledgments. RC acknowledges the support of the Office of Naval Research. VG thanks Faculty of Mechanical Engineering, Technion, for hospitality during his sabbatical. AZ gratefully acknowledges funding from the US Army DEVCOM Army Research Office through contract nr. W911NF-22-2-0256 and from the European Union through Horizon Europe ERC Grant number: 101043968 “Multimech”. We thank Prof. David S. Simmons for providing simulation data.

The authors declare no competing financial interests.

- [1] C. A. Angell, Formation of glasses from liquids and biopolymers, *Science* (1979) **267**, 1924 (1995).
- [2] C. A. Angell, Complex Behavior of Glassy Systems, Springer Lecture Notes in Physics **402**, (1997).
- [3] C. A. Angell, Glassforming liquids with microscopic to macroscopic two-state complexity, *Progress of Theoretical Physics Supplement* 1 (1997).
- [4] C. A. Angell, Relaxation in liquids, polymers and plastic crystals—strong/fragile patterns and problems, *J Non Cryst Solids* **131**, 13 (1991).
- [5] L. Berthier and M. D. Ediger, Facets of glass physics, *Phys Today* **69**, 40 (2016).

- [6] M. D. Ediger and P. Harrowell, Perspective: Supercooled liquids and glasses, *J Chem Phys* **137**, 080901 (2012).
- [7] A. Zaccone, *Theory of Disordered Solids: From Atomistic Dynamics to Mechanical, Vibrational, and Thermal Properties*, Vol. 1015 (Springer Nature, 2023).
- [8] J. C. Dyre, Source of non-Arrhenius average relaxation time in glass-forming liquids, *J Non Cryst Solids* **235**, 142 (1998).
- [9] J. C. Dyre, Colloquium: The glass transition and elastic models of glass-forming liquids, *Rev. Mod. Phys.* **78**, 953 (2006).
- [10] J. C. Dyre, Solid-that-flows picture of glass-forming liquids, *J Phys Chem Lett* **15**, 1603 (2024).
- [11] G. B. McKenna and S. L. Simon, 50th anniversary perspective: Challenges in the dynamics and kinetics of glass-forming polymers, *Macromolecules* **50**, 6333 (2017).
- [12] C. B. Roth, *Polymer Glasses* (CRC Press, 2016).
- [13] H. Vogel, Das temperaturabhängigkeitsgesetz der viskosität von flüssigkeiten, *Phys. Z.* **22**, 645 (1921).
- [14] G. S. Fulcher, Analysis of recent measurements of the viscosity of glasses, *Journal of the American Ceramic Society* **8**, 339 (1925).
- [15] G. Tammann and W. Hesse, The dependence of viscosity upon the temperature of supercooled liquids, *Z. Anorg. Allg. Chem* **156**, 245 (1926).
- [16] G. Adam and J. H. Gibbs, On the temperature dependence of cooperative relaxation properties in glass-forming liquids, *J Chem Phys* **43**, 139 (1965).
- [17] A. K. Doolittle, Studies in Newtonian flow. II. The dependence of the viscosity of liquids on free-space, *J Appl Phys* **22**, 1471 (1951).
- [18] G. B. McKenna and J. Zhao, Accumulating evidence for non-diverging time-scales in glass-forming fluids, *J Non Cryst Solids* **407**, 3 (2015).

- [19] H. Yoon and G. B. McKenna, Testing the paradigm of an ideal glass transition: Dynamics of an ultrastable polymeric glass, *Sci Adv* **4**, eaau5423 (2018).
- [20] J. Zhao and G. B. McKenna, The apparent activation energy and dynamic fragility of ancient ambers, *Polymer (Guildf)* **55**, 2246 (2014).
- [21] O.-V. Laukkanen and H. H. Winter, The dynamic fragility and apparent activation energy of bitumens as expressed by a modified Kaelble equation, *J Non Cryst Solids* **499**, 289 (2018).
- [22] I. Avramov and A. Milchev, Effect of disorder on diffusion and viscosity in condensed systems, *J Non Cryst Solids* **104**, 253 (1988).
- [23] J. C. Mauro, Y. Yue, A. J. Ellison, P. K. Gupta, and D. C. Allan, Viscosity of glass-forming liquids, *Proceedings of the National Academy of Sciences* **106**, 19780 (2009).
- [24] V. Ginzburg, A simple mean-field model of glassy dynamics and glass transition, *Soft Matter* **16**, 810 (2020).
- [25] M. Ozawa and G. Biroli, Elasticity, facilitation, and dynamic heterogeneity in glass-forming liquids, *Phys Rev Lett* **130**, 138201 (2023).
- [26] M. Sellitto, Cooperative heterogeneous facilitation: Multiple glassy states and glass-glass transition, *Physical Review E—Statistical, Nonlinear, and Soft Matter Physics* **86**, 030502 (2012).
- [27] A. S. Keys, J. P. Garrahan, and D. Chandler, Calorimetric glass transition explained by hierarchical dynamic facilitation, *Proceedings of the National Academy of Sciences* **110**, 4482 (2013).
- [28] T. Speck, Dynamic facilitation theory: a statistical mechanics approach to dynamic arrest, *Journal of Statistical Mechanics: Theory and Experiment* **2019**, 084015 (2019).
- [29] C. Herrero and L. Berthier, Direct numerical analysis of dynamic facilitation in glass-forming liquids, *Phys Rev Lett* **132**, 258201 (2024).

- [30] F. W. Starr, J. F. Douglas, and S. Sastry, The relationship of dynamical heterogeneity to the Adam-Gibbs and random first-order transition theories of glass formation, *Journal of Chemical Physics* **138**, (2013).
- [31] T. R. Kirkpatrick and D. Thirumalai, Colloquium: Random first order transition theory concepts in biology and physics, *Rev Mod Phys* **87**, (2015).
- [32] D. R. Reichman and P. Charbonneau, Mode-coupling theory, *Journal of Statistical Mechanics: Theory and Experiment* **2005**, P05013 (2005).
- [33] T. R. Kirkpatrick, Mode-coupling theory of the glass transition, *Phys Rev A (Coll Park)* **31**, 939 (1985).
- [34] S. P. Das, Mode-coupling theory and the glass transition in supercooled liquids, *Rev Mod Phys* **76**, 785 (2004).
- [35] L. M. C. Janssen, Mode-coupling theory of the glass transition: A primer, *Front Phys* **6**, 97 (2018).
- [36] A. D. Phan and K. S. Schweizer, Elastically Collective Nonlinear Langevin Equation Theory of Glass-Forming Liquids: Transient Localization, Thermodynamic Mapping, and Cooperativity, *Journal of Physical Chemistry B* **122**, 8451 (2018).
- [37] Y. Zhou, B. Mei, and K. S. Schweizer, Activated relaxation in supercooled monodisperse atomic and polymeric WCA fluids: Simulation and ECNLE theory, *J. Chem. Phys.* **156**, 114901 (2022).
- [38] J. F. Douglas and W.-S. Xu, Equation of state and entropy theory approach to thermodynamic scaling in polymeric glass-forming liquids, *Macromolecules* **54**, 3247 (2021).
- [39] J. Dudowicz, K. F. Freed, and J. F. Douglas, Generalized entropy theory of polymer glass formation, *Adv Chem Phys* **137**, 125 (2008).
- [40] W.-S. Xu, J. F. Douglas, W. Xia, and X. Xu, Understanding Activation Volume in Glass-Forming Polymer Melts via Generalized Entropy Theory, *Macromolecules* **53**, 7239 (2020).

- [41] R. P. White and J. E. G. Lipson, The cooperative free volume rate model for segmental dynamics: Application to glass-forming liquids and connections with the density scaling approach*, The European Physical Journal E **42**, 100 (2019).
- [42] R. P. White and J. E. G. Lipson, Polymer free volume and its connection to the glass transition, Macromolecules **49**, 3987 (2016).
- [43] R. P. White and J. E. G. Lipson, Explaining the T, V-dependent dynamics of glass forming liquids: The cooperative free volume model tested against new simulation results, J Chem Phys **147**, 184503 (2017).
- [44] V. Ginzburg, Combined description of polymer PVT and relaxation data using a dynamic “SL-TS2” mean-field lattice model, Soft Matter **17**, 9094 (2021).
- [45] V. Ginzburg, Modeling the Glass Transition of Free-Standing Polymer Thin Films Using the “SL-TS2” Mean-Field Approach, Macromolecules **55**, 873 (2022).
- [46] V. V Ginzburg, A. Zacccone, and R. Casalini, Combined Description of Pressure-Volume-Temperature and Dielectric Relaxation of Several Polymeric and Low-Molecular-Weight Organic Glass-Formers using ‘SL-TS2’ Mean-Field Approach, Soft Matter **18**, 8456 (2022).
- [47] V. V Ginzburg, E. Fazio, and C. Corsaro, Combined Description of the Equation of State and Diffusion Coefficient of Liquid Water Using a Two-State Sanchez–Lacombe Approach, Molecules **28**, 2560 (2023).
- [48] V. V Ginzburg, O. V Gendelman, and A. Zacccone, Unifying Physical Framework for Stretched-Exponential, Compressed-Exponential, and Logarithmic Relaxation Phenomena in Glassy Polymers, Macromolecules **57**, 2520 (2024).
- [49] K. Kunal, C. G. Robertson, S. Pawlus, S. F. Hahn, and A. P. Sokolov, Role of chemical structure in fragility of polymers: a qualitative picture, Macromolecules **41**, 7232 (2008).

- [50] B. Schmidtke, M. Hofmann, A. Lichtinger, and E. A. Rössler, Temperature dependence of the segmental relaxation time of polymers revisited, *Macromolecules* **48**, 3005 (2015).
- [51] A. Kudlik, S. Benkhof, T. Blochowicz, C. Tschirwitz, and E. Rössler, The dielectric response of simple organic glass formers, *J Mol Struct* **479**, 201 (1999).
- [52] Th. Blochowicz, C. Gainaru, P. Medick, C. Tschirwitz, and E. A. Rössler, The dynamic susceptibility in glass forming molecular liquids: The search for universal relaxation patterns II, *J. Chem. Phys.* **124**, 134503 (2006).
- [53] J. Hintermeyer, A. Herrmann, R. Kahlau, C. Goiceanu, and E. A. Rössler, Molecular Weight Dependence of Glassy Dynamics in Linear Polymers Revisited, *Macromolecules* **41**, 9335 (2008).
- [54] R. Casalini, A. W. Snow, and C. M. Roland, Temperature dependence of the Johari–Goldstein relaxation in poly (methyl methacrylate) and poly (thiomethyl methacrylate), *Macromolecules* **46**, 330 (2013).
- [55] C. Liu J, Y. He, C. Keunings, and R. Bailly, New linearized relation for the universal viscosity-temperature behavior of polymer melts, *Macromolecules* **39**, 8867 (2006).
- [56] K. Kunal, M. Paluch, C. M. Roland, J. E. Puskas, Y. Chen, and A. P. Sokolov, Polyisobutylene: A most unusual polymer, *J Polym Sci B Polym Phys* **46**, 1390 (2008).
- [57] J. Zhao and G. B. McKenna, Temperature divergence of the dynamics of a poly (vinyl acetate) glass: Dielectric vs. mechanical behaviors, *J Chem Phys* **136**, 154901 (2012).
- [58] W. Heinrich and B. Stoll, Dielectric investigation of the glass relaxation in poly (vinyl acetate) and poly (vinyl chloride) under high hydrostatic pressure, *Colloid Polym Sci* **263**, 873 (1985).
- [59] C. M. Roland and R. Casalini, Dynamics of Poly(cyclohexyl methacrylate): Neat and in Blends with Poly(α -methylstyrene), *Macromolecules* **40**, 3631 (2007).
- [60] D. Huang and G. B. McKenna, New insights into the fragility dilemma in liquids, *J Chem Phys* **114**, 5621 (2001).

- [61] J. M. Caruthers and G. A. Medvedev, Quantitative model of super-Arrhenian behavior in glass forming materials, *Phys Rev Mater* **2**, 55604 (2018).
- [62] M. Reiner, The deborah number, *Phys Today* **17**, 62 (1964).
- [63] B. A. Pazmiño Betancourt, J. F. Douglas, and F. W. Starr, String model for the dynamics of glass-forming liquids, *Journal of Chemical Physics* **140**, 204509 (2014).
- [64] B. A. Pazmiño Betancourt, P. Z. Hanakata, F. W. Starr, and J. F. Douglas, Quantitative relations between cooperative motion, emergent elasticity, and free volume in model glass-forming polymer materials, *Proc. Natl. Acad. Sci. U.S.A.* **112**, 2966 (2015).
- [65] D. S. Simmons and J. F. Douglas, Nature and interrelations of fast dynamic properties in a coarse-grained glass-forming polymer melt, *Soft Matter* **7**, 11010 (2011).
- [66] J.-H. Hung, T. K. Patra, V. Meenakshisundaram, J. H. Mangalara, and D. S. Simmons, Universal localization transition accompanying glass formation: insights from efficient molecular dynamics simulations of diverse supercooled liquids, *Soft Matter* **15**, 1223 (2019).
- [67] R. W. Hall and P. G. Wolynes, The aperiodic crystal picture and free energy barriers in glasses, *J Chem Phys* **86**, 2943 (1987).

Supporting Information for:

Universality of Alpha-Relaxation in Glasses

Valeriy V. Ginzburg¹, Oleg Gendelman², Riccardo Casalini³, and Alessio Zaccone⁴

¹Department of Chemical Engineering and Materials Science, Michigan State University, East Lansing, Michigan, USA 48824

²Faculty of Mechanical Engineering, Technion, Haifa 32000003, Israel

³Chemistry Division, Naval Research Laboratory, 4555 Overlook Avenue SW, Washington, D.C., USA 20375

⁴University of Milan, Department of Physics, via Celoria 16, 20133 Milano, Italy

1. Parameter table for the glass-formers

Table S 1. Model parameters for the 34 glass-formers. See text for details

Material	T_g , K	T_∞/T_g	T_∞ , K	$\log(\tau_\infty, s)$	m	T_A , K	$\log(\tau_A, s)$
Silica	1475	0.748	1104	-14.8	23.5	1352.61	2.9
Window Glass	833	0.787	655	-16.2	31.4	803.04	1.5
Corning Aluminosilicate	1050	0.787	826	-16.2	31.4	1012.24	1.5
Basalt	993	0.819	813	-17.6	42.7	996.36	0.1
Glycerol	191	0.869	166	-21.0	74.5	203.50	-3.3
PDMS	144	0.911	131	-25.5	117.9	160.80	-7.8
PBD	180	0.878	158	-21.8	82.2	193.70	-4.1
PS	373	0.896	334	-23.6	100.2	409.51	-5.9
PMMA	378	0.896	339	-23.6	100.2	415.00	-5.9
PC	423	0.896	379	-23.6	100.2	464.40	-5.9
PVC	350	0.914	320	-25.8	121.2	392.02	-8.1
PVAc	307	0.875	269	-21.6	79.8	329.38	-3.9
PCHMA	354	0.861	305	-20.3	67.5	373.41	-2.6
PIB	198	0.799	158	-16.7	35.0	193.76	1.1
3MP	80	0.925	74	-27.4	135.2	90.69	-9.7
n-Propanol	98	0.898	88	-23.9	102.5	107.85	-6.2
EC	104	0.875	91	-21.5	79.4	111.52	-3.8
3BP	108	0.870	94	-21.1	75.3	115.20	-3.4
EB	115	0.870	100	-21.1	74.6	122.55	-3.3
Toluene	117	0.855	100	-19.9	63.1	122.55	-2.1
Cumene	129	0.876	113	-21.6	80.3	138.49	-3.9
PC	158	0.854	135	-19.8	62.9	165.45	-2.1
DP	181	0.884	160	-22.4	87.8	196.09	-4.7
MTD	187	0.882	165	-22.2	86.3	202.21	-4.5
DMP	191	0.890	170	-23.0	94.0	208.34	-5.3
TPP	200	0.900	180	-24.1	104.8	220.60	-6.4
OBP	220	0.886	195	-22.6	90.2	238.98	-4.9
Salol	221	0.869	192	-21.0	74.0	235.30	-3.3
OTP	243	0.893	217	-23.3	97.1	265.94	-5.6
Sorbitol	268	0.896	240	-23.6	99.8	294.13	-5.9
Glucose	312	0.865	270	-20.7	71.2	330.89	-3.0
CPDE	312	0.875	273	-21.5	79.4	334.57	-3.8
TNB	342	0.906	310	-24.9	112.2	379.91	-7.2
B2O3	530	0.849	450	-19.5	59.2	551.49	-1.7

2. Parameter table for the universal TS2 and SL-TS2 Models

Table S 2. Parameters for the universal TS2 and SL-TS2 models.

TS2 Parameters	
E_1/RT_x	50 (± 5)
E_2/RT_x	150 (± 10)
$\Delta S/R$	16 (± 1)
SL-TS2 Parameters	
α_{LL}	0.934 (± 0.005)
r_s	388 (± 3)
r_L	412 (± 3)

3. Shifted log-log plots for the a-relaxation time vs. temperature for various molecular glasses

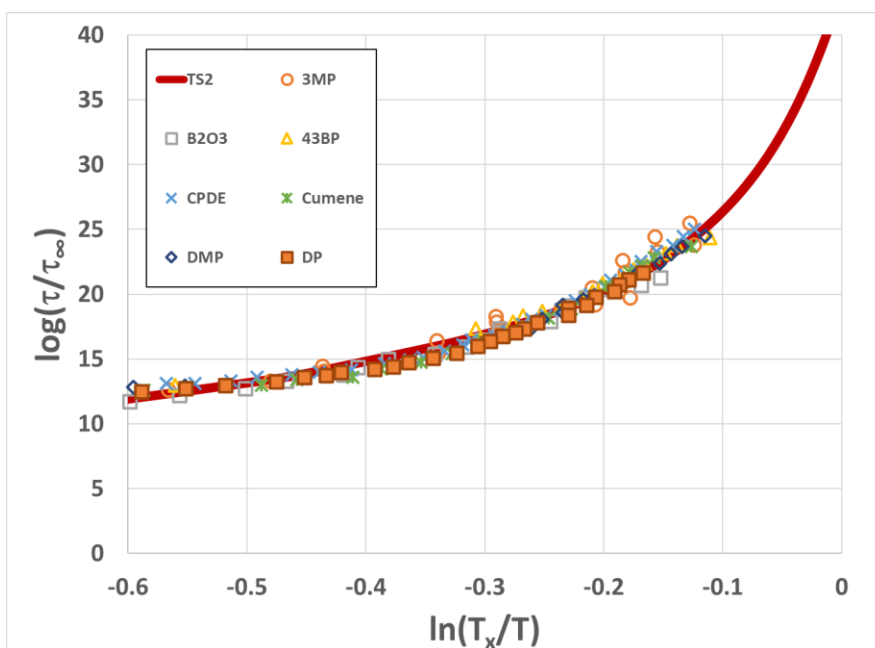


Figure S 1. Log-log plot of scaled relaxation time vs. scaled temperature for a subset of molecular glass-formers. TS2 is the universal TS2 model curve, B2O3 is boron oxide, 3MP is 3-methyl pentane; 43BP is 4,3-bromopentane; CPDE is cresolphthalein-dimethylether; DMP is dimethyl phthalate; DP is diethyl phthalate.

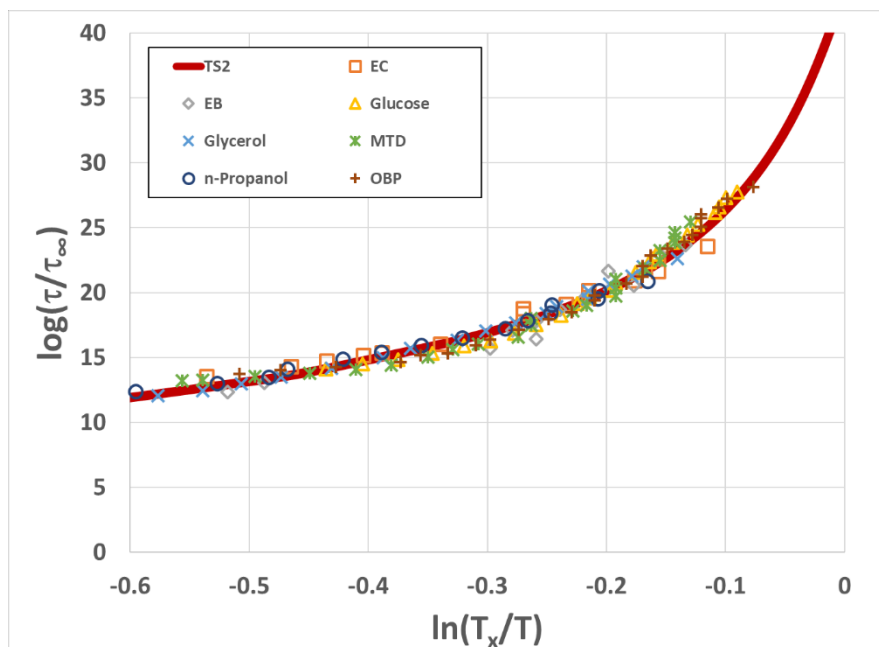


Figure S 2. Same as Figure S1, but with a different subset of molecular glasses. Abbreviations: EC – ethyl cyclohexane; EB is ethylbenzene; MTD is *m*-toluidine; OBP is *o*-benzylphenol, also known as α -phenyl-*o*-cresol.

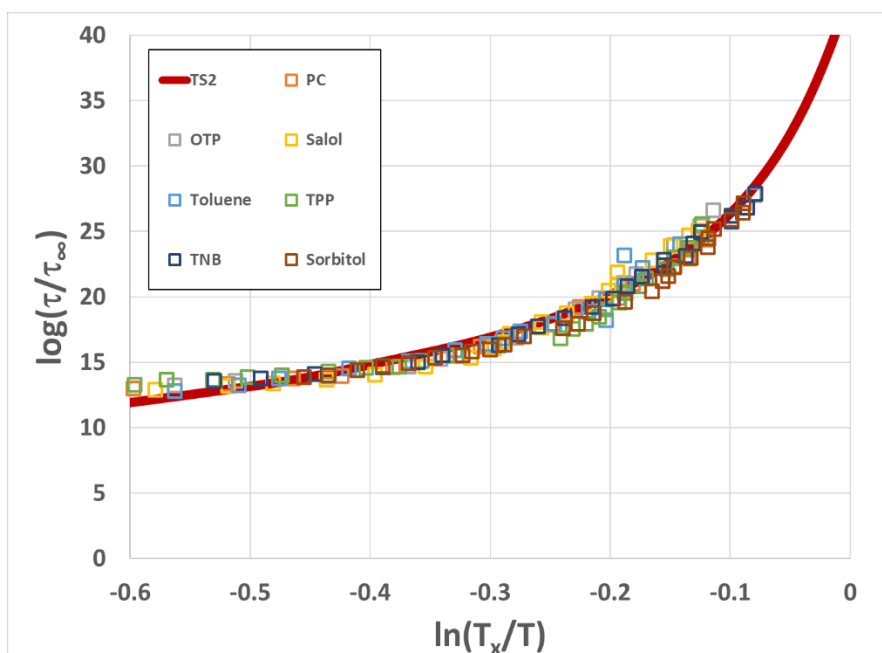


Figure S 3. Same as Figures S1 – S2, but with a different subset of molecular glasses. Abbreviations: PC – propylene carbonate; OTP – ortho-terphenyl; TPP – triphenyl phosphite; TNB – tri- α -naphthyl benzene.

4. Relationship between fragility and Arrhenius relaxation time

The fragility within TS2 can be evaluated as,

$$m = \frac{\partial \log(\tau_\alpha)}{\partial \left[\frac{T_g}{T} \right]_{T=T_g}} = \frac{1}{\ln(10)} \frac{T_x}{T_g} \left[\overline{E}_1 + (\overline{E}_2 - \overline{E}_1) \psi_g + \frac{T_x}{T_g} (\overline{E}_2 - \overline{E}_1) S \psi_g (1 - \psi_g) \right] \quad (\text{S1})$$

Where $S \equiv \Delta S/R$, and

$$\psi_g = \left[1 + \exp \left(S \left[\frac{T_x}{T_g} - 1 \right] \right) \right]^{-1} \quad (\text{S2})$$

The relaxation time at $T = T_A$ is given by,

$$\log \left(\frac{\tau_g}{\tau_A} \right) = \frac{1}{\ln(10)} \left[\overline{E}_1 \left(\frac{T_x}{T_g} - \frac{T_x}{T_A} \right) + (\overline{E}_2 - \overline{E}_1) \left(\frac{T_x}{T_g} \psi_g - \frac{T_x}{T_A} \psi_A \right) \right] \quad (\text{S3})$$

As discussed in the main manuscript, the ratio T_x/T_A is a universal constant once we have chosen $\psi_A = 0.05$; $T_x/T_A = Q = 0.816$. Recalling that $\log(\tau_g) = 2$, we can express $\log(\tau_A)$ as a function of a single unknown, T_x/T_g ,

$$\log(\tau_A) = 2 - \frac{1}{\ln(10)} \left[\overline{E}_1 \left(\frac{T_x}{T_g} - Q \right) + (\overline{E}_2 - \overline{E}_1) \left(\frac{T_x}{T_g} \psi_g - Q \psi_A \right) \right] \quad (\text{S4})$$

Note that ψ_g is given by equation S2 and is thus also a function of T_x/T_g . We can solve equation S4 numerically to express T_x/T_g as a function of $\log(\tau_A)$, and then substitute into equation S1 to determine the relationship between m and $\log(\tau_A)$, as plotted in Figure 3b of the main manuscript. Below, in Figure S4, we re-plot the data from Figure 3b and fit $\log(\tau_A)$ vs. m using a fifth-order polynomial function.

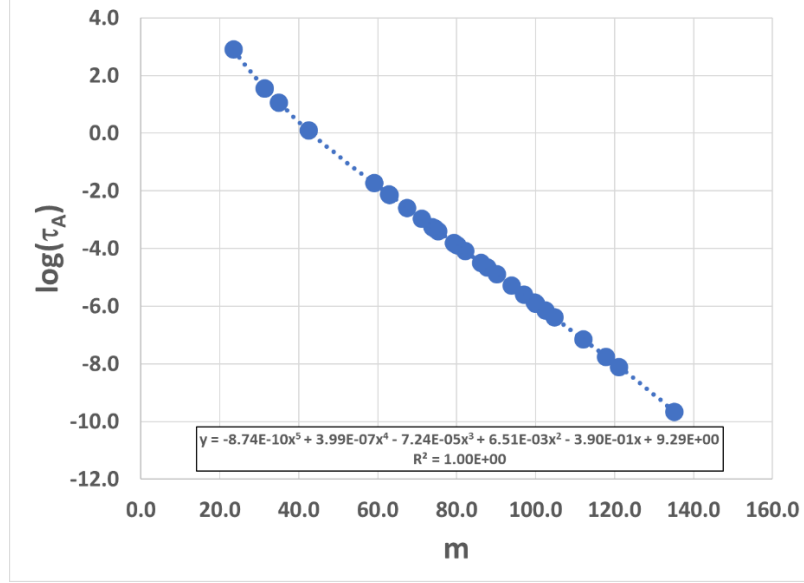


Figure S 4. Logarithm of the Arrhenius relaxation time as a function of fragility – the data for all 34 glass-formers and the fifth-order polynomial fit.

5. Functional form for TS2 relaxation time relative to the Arrhenius time and Arrhenius temperature

The universal TS2 relaxation time as a function of temperature is given by,

$$\log\left(\frac{\tau_\alpha[X]}{\tau_\infty}\right) = \frac{1}{\ln(10)} \left[\frac{\bar{E}_1}{X} + \frac{\bar{E}_2 - \bar{E}_1}{X} \psi[X] \right] \quad (\text{S5})$$

Where $X = T/T_X$ and $\psi[X] = \left\{ 1 + \exp\left[\frac{\Delta S}{R}(1 - X^{-1})\right] \right\}^{-1}$. Given the definition of the Arrhenius

temperature as the temperature for which $\psi = \psi_A = 0.05$, we can easily find $X_A = T_A/T_X$,

$$X_A = 1 - \frac{1}{S} \ln\left(\frac{1}{\psi_A} - 1\right) \approx 0.816 \quad (\text{S6})$$

Thus,

$$\log\left(\frac{\tau_\alpha[Z]}{\tau_A}\right) = \frac{1}{\ln(10)} \left[\frac{\bar{E}_1}{X_A} (Z^{-1} - 1) + \frac{\bar{E}_2 - \bar{E}_1}{X_A} (\psi[Z] Z^{-1} - \psi_A) \right] \quad (\text{S7})$$

Where $Z = T/T_A$.

